Cancer Nanotechnology

RESEARCH Open Access

The effects of peptide IF7-conjugated dendrimer loaded with doxorubicin on colorectal cancer

Omid Reza Tamtaji[1], Mehdi Shafiee Ardestani[2,3], Abdolkarim Talebi Taheri[4], Michael R. Hamblin[5], Tina Rahjoo[1], Fatemeh Nabavizadeh[6*] and Hamed Mirzaei[7*]

*Correspondence:
Nabavizadeh@tums.ac.ir;
h.mirzaei2002@gmail.com

[1] Department of Physiology, School of Medicine, Tehran University of Medical Sciences, Tehran, Islamic Republic of Iran
[2] Department of Radio Pharmacy, Faculty of Pharmacy, Tehran University of Medical Sciences, Tehran, Islamic Republic of Iran
[3] Research Center for Nuclear Medicine, Shariati Hospital, North Kargar Ave. 1411713135, Tehran, Iran
[4] Department of Clinical Biochemistry, School of Medicine, Tehran University of Medical Sciences, Tehran, Islamic Republic of Iran
[5] Laser Research Centre, Faculty of Health Science, University of Johannesburg, Doornfontein 2028, South Africa
[6] Electrophysiology Research Center, Neuroscience Institute, Tehran University of Medical Sciences, Tehran, Islamic Republic of Iran
[7] Research Center for Biochemistry and Nutrition in Metabolic Diseases, Kashan University of Medical Sciences, Kashan, Islamic Republic of Iran

Abstract

We assessed the therapeutic potential of a combination of dendrimer generation 2 (G2) + doxorubicin (DOX) + peptide IF7 on colorectal cells. The researchers utilized regular examinations to assess the dimensions, structure, distribution, and dosage of DOX in the manufactured nanoparticles through physical and chemical evaluations. Afterwards, the MTT (3-(4,5-dimethylthiazolyl-2)-2,5-diphenyltetrazolium bromide) test was used to evaluate how the presence of these nanoparticles affected the ability of HCT116 cells to survive. Finally, both reverse transcription–quantitative polymerase chain reaction (RT–qPCR) and Western blotting methods were used to measure the levels of gene expression in the Wnt/β-catenin signaling pathway, which includes genes, such as β-catenin, cyclin D1, Twist, and Zinc-finger E-box-binding homeobox 1 (ZEB1). In addition, protein expression related to apoptosis (B-cell lymphoma 2 (Bcl2), BCL2 associated X (Bax), and caspase-3) and angiogenesis (vascular endothelial growth factor (VEGF)) was also assessed. The dendrimer G2 + DOX + IF7 had a mean diameter of 165.6 nm, displayed primarily a round form, and had the capability to react to variations in acidity levels. The mixture of dendrimer G2 + DOX + IF7 demonstrated a notable capacity to damage the HCT116 cell line by diminishing the expression of β-catenin, cyclin D1, Twist, and ZEB1 genes. Moreover, it decreased the amounts of VEGF and Bcl2 proteins and increased the levels of Bax and caspase-3 proteins. In conclusion, this combination has an ability to trigger cell death by precisely directing the Wnt/β-catenin and apoptosis pathways.

Keywords: Colorectal cancer, Dendrimer, Annexin A1, Doxorubicin, Apoptosis, Wnt signaling

Introduction

Colorectal cancer (CRC) is a significant worry for the overall health of the global population and is currently the second leading cause of death from cancer (Xi and Xu 2021). It is not solely determined by genetic factors whether someone will develop colon cancer or not. Other external factors, such as alterations in diet and overall way of living, also have a significant impact (Barot et al. 2024; Kato and Sun 2023). The onset of colon

cancer occurs when cells experience excessive growth due to molecular mechanisms, including the Wnt/β-catenin pathway and programmed cell death (Boopathy et al. 2024). Doxorubicin (DOX) along with other commonly utilized chemotherapy medications play a crucial role in managing advanced cancer. DOX's ability to inhibit cancer can be credited to various mechanisms, such as its attachment to DNA and inhibition of topoisomerase II, leading to the destruction of cancer cells (Minotti et al. 2004). Furthermore, it specifically targets various molecules and cells, resulting in a variety of harmful consequences. For instance, it triggers the activation of adenosine monophosphate (AMP)-activated protein kinase, ultimately leading to the death of cells. This process alters the ratio of B-cell lymphoma 2 (Bcl2) and BCL2 associated X (Bax) proteins, resulting in the activation of various caspases that ultimately induce apoptosis (Tacar et al. 2013). Lüpertz et al. (2010) showed that DOX caused cells in the G0/G1 stage of the cell cycle to stop dividing, ultimately leading to the death of CRC cells through apoptosis. Moreover, the heightened presence of p21 was discovered to be linked to the sensitivity of CRC cells to DOX (Ravizza et al. 2004). It blocks the activity of the Wnt/β-catenin signaling pathway and triggers cell death in colorectal cancer cells (Rajabi et al. 2024). Furthermore, blocking the activity of WNT signaling increases the susceptibility of cancer cells to DOX (Suebsoonthron et al. 2017). Although DOX has the capability to concentrate on specific tumors, its effectiveness is restricted and it has the potential to negatively impact healthy cells due to its poisonous properties (Corrie 2008). An instance of this would be the induction of heart toxicity over time as a potential negative consequence of DOX usage (Wang 2024).

The advancements in nanotechnology have led to continuous enhancements in contemporary chemotherapy techniques, leading to improved efficiency and minimized adverse effects through the usage of targeted treatments and drug delivery systems (Victoir et al. 2024). Extensive research has been conducted on dendrimers as a highly efficient method for resolving the aforementioned problems in drug delivery (Rastogi et al. 2024). Dendrimers are precisely engineered and synthesized large molecules with a well-organized and uniform branching structure (Abbasi et al. 2014). The effectiveness of the dendrimers in binding and enclosing hydrophobic chemotherapy drugs, ultimately improving their water solubility and bioavailability, heavily relies on their hydrophobic interior environment. As a result, this has a positive impact on reducing the adverse reactions caused by DOX (Morgan et al. 2006; Morgan et al. 2003; Zhang et al. 2014a). The combination of dendrimer–DOX can greatly promote the occurrence of apoptosis through the formation of complexes, as it has the capability to spontaneously arrange into tiny particles and ultimately leading to powerful anti-cancer properties (Zhang et al. 2014a). Although dendrimers have high advantages (Astruc et al. 2010; Zhao et al. 2010; Cheng and Xu 2008), the design of specific ligand-modified dendrimer nanocarriers can improve the targeting efficacy of dendrimers, and thus improve the treatment efficiency of chemotherapy drugs, furthermore (Yang 2016; Hsu et al. 2017). The expression of Annexin A1 (ANXA1) significantly increases in malignant cells, particularly in the endothelium of blood vessels, in both colorectal cancer (CRC) and other forms of cancer (Su et al. 2010; Biaoxue et al. 2012; Okano et al. 2015). Numerous research investigations have shown that the arrangement of amino acids, known as IF7 or IFLLWQR, is capable of attaching to the primary segment of the ANXA1 protein (Hatakeyama et al. 2011;

Hatakeyama et al. 2009; Nonaka et al. 2020). When drugs combined with IF7 are employed, they greatly gather on the exterior surface of cancerous endothelial cells (Hatakeyama et al. 2011). The advancement of breast tumors is effectively prevented through the use of nanoparticles that have been accurately guided with the IF7 peptide and filled with paclitaxel (Yu et al. 2015). Furthermore, the IF7 peptide-SN38 has the ability to efficiently pass through the protective barrier of the blood–brain barrier, thus inhibiting the growth of brain tumors (Nonaka et al. 2020).

As a result, considering all the reasons provided, we carried out an investigation in which we synthesized G2 dendrimer nanoparticles with IF7 peptide and doxorubicin in a specific manner, and thoroughly analyzed their characteristics. Moreover, we evaluated the effect of these tiny particles on the HCT116 colorectal cancer cells, specifically looking at their potential for causing cell death and how they may affect the Wnt/β-catenin, angiogenesis, and apoptosis processes.

Materials and methods

Preparation of dendrimer G2 targeted with IF7 peptide containing doxorubicin

Preparation of nano-dendrimer G2

A dendrimer with a linear and spherical structure, named G2 and possessing a negative charge, was created by mixing together 1 mL (3.7 mmol) of polyethylene glycol 600, 10 mL of dimethyl sulfoxide, 0.75 g (2*3.7 mmol) of *N*,*N*′-dicyclohexylcarbodiimide, and 0.71 g (2*3.7 mmol) of citric acid, following methods outlined in previous research (Mohammadzadeh et al. 2017; Namazi and Adeli 2005) (Fig. 1).

Peptide conjugation

To begin, Dendrimer G2 nanoparticles were submerged in a mixture comprising of double deionized water (DW), as well as 30 mg of 1-Ethyl-3-(3-dimethylaminopropyl) carbodiimide (EDC) and 24 mg of *N*-Hydroxysuccinimide (NHS). After that, the combination was agitated at normal room temperature for a period of 1 h. This was followed by the removal of any excess EDC and NHS through the process of dialysis,

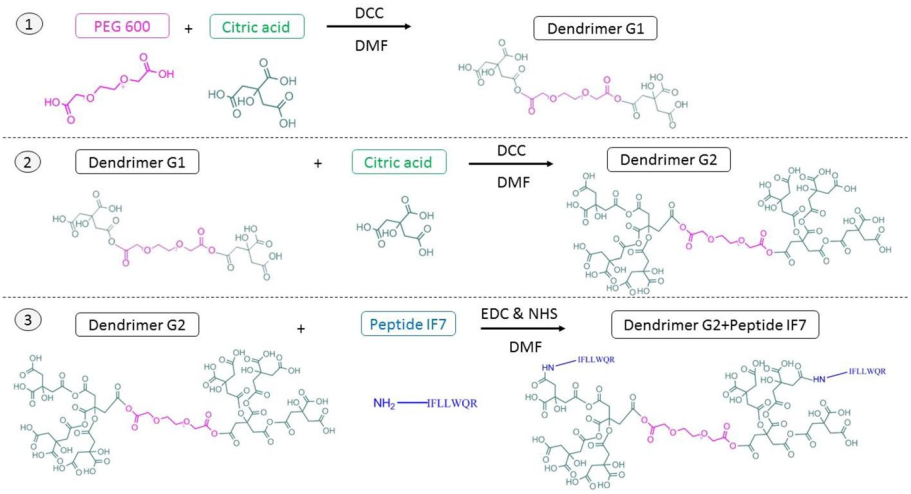

Fig. 1 Schematic illustration of synthesis of dendrimer G2 + peptide IF7

which lasted for 1 h. At the same time, the IF7 peptide produced by Pepmic Company in China, containing the sequence of amino acid IFLLWQR, was mixed with distilled water and exposed to a temperature of 85 °C for a period of 2 min. After being allowed to come to room temperature, the previously reacted dendrimer G2 was mixed with the peptide at a ratio of 1:1. After being sonicated for a full 10 min, the peptides were then dialyzed against room temperature DW for a period of 2 h to remove any remaining unreacted peptides (Fig. 1).

Doxorubicin loading

To load DOX into the prepared dendrimers, 5 mg of excess Doxorubicin was combined with 10 mg of dendrimer G2 + IF7 using mass ratios of approximately 1 mg Doxorubicin: 10 mg dendrimer G2 + IF7 and 1 mg Doxorubicin: 2 mg dendrimer G2. Once the components were combined, the resulting blend was then placed in an orbital shaker/incubator and agitated for 10 min at a cool temperature of 4 °C. To eliminate any leftover DOX that was not taken in, the combination was subjected to dialysis for 48 h using a 20,000 Da cutoff dialysis bag in 1 × 1 L of deionized water. A graph was produced to evaluate the effectiveness of loading DOX, which was then followed by the generation of DOX solutions at varying levels of concentration. To determine the proportion of DOX that was not loaded, the UV–Vis absorption spectrophotometer measured the absorbance at 494 nm. The sample's loading efficiency (LE) was determined using the following mathematical equation:

$$\text{Loading efficiency (LE)} = \frac{\text{amount of total loaded drug}}{\text{total amount of nanoparticle}} \times 100.$$

Characterization of prepared nanoparticles

Researchers employed a Fourier Transform Infrared Spectroscopy (FTIR) analysis using a spectrum of two spectrophotometers (45° ZnSe crystal, PerkinElmer Inc., US), within the range of 1000–4000 cm^{-1} according to the E1252-98 (2021) guideline to confirm that the combination of dendrimer G2 and peptide IF7 was accomplished. Dynamic light scattering (DLS) and the Nano Zetasizer (Malvern Instruments, UK) were utilized to analyze the dimensions and electric charge of the mixtures based on the guidance of E2865-12 (2018). A comprehensive examination was conducted on the structure of the prepared formulations using established procedures, utilizing both transmission electron microscopy (TEM, ZEISS, Germany) and field emission scanning electron microscopy (FESEM; ZEISS, Germany) according to the E2578-07 (2018) and ISO 16,700:2016 guidelines. Photographs were obtained using a Gatan SC1000 camera.

Cell culture

The HCT116 cells (ANXA1 positive), and SW480 cells (ANXA1 negative), derived from human colon cancer cells, and Human Foreskin Fibroblast cells (HFF-2) were generously provided by the Pasteur Institute in Tehran, Iran. The cells were grown in Dulbecco's Modified Eagle Medium (DMEM) solution and enriched with 1% penicillin–streptomycin and 10% fetal bovine serum that had been rendered inactive through heat treatment. Furthermore, the cells were submerged in a moist environment containing

5% carbon dioxide and 95% air while being kept at a steady temperature of 37 degrees Celsius. The nutrient-rich environment was refreshed every 48–72 h.

MTT (3-(4, 5-dimethylthiazolyl-2)−2, 5-diphenyltetrazolium bromide) assay

For the study, 10,000 HCT116 cells were equally spread into each well of a 96-well plate and allowed to multiply for 24 h. Later on, the original DMEM medium was substituted with a new one containing varying doses of DOX, dendrimer G2, dendrimer G2 + DOX, and dendrimer G2 + DOX + IF7. After being exposed to a controlled environment for an entire day, the cells were additionally treated with 20 µL of a 5 mg/mL MTT solution for a duration of 3 h. Next, 100 µL of Dimethyl sulfoxide (DMSO) was substituted for the MTT medium. After 30 min, the solution was examined for its absorbance of blue formazan using a microplate reader (Biotech, MQX200) set at 570 nm. This measurement was used to determine the half-maximal inhibitory concentration (IC50) value.

Reverse transcription–quantitative polymerase chain reaction (RT–qPCR)

The total RNA was extracted from cells in all the groups using the TRIzol reagent as per the manufacturer's instructions. Afterwards, the RNA molecule was broken down through the use of RNase-free DNase I. To produce complementary single-stranded DNA, the PrimeScript RT Reagent Kit was utilized. After that, the process of RT-qPCR was used by Ampliqon master mix on StepOne Plus RT-PCR system to amplify the complementary DNA. The thermal cycling process included specific parameters, beginning with a 5-min initial heating step at 95°C and ending with a 5-min final extension step at 72 °C. Following that, a heat treatment was carried out consisting of exposure to a heat of 95 °C for 20 s, followed by a temperature of 68 °C for 20 s, and finally 72 °C for 30 s. The primers utilized were specifically chosen from Primer Bank, which can be found in Table 1.

Western blot

A Western blot analysis was carried out with the aim of identifying any alterations in the levels of Bax, Caspase-3, Bcl-2, and vascular endothelial growth factor (VEGF) proteins within the cancerous cells. The cells were ruptured using a cell lysis buffer, for a period of 20 min at a temperature of 4 °C. Following a 30-min exposure to ice, the mixture was

Table 1 Sequence of the used primers

Gene	Sequence
ZEB1-F	GCACCTGAAGAGGACCAGAG
ZEB1-R	TGCATCTGGTGTTCCATTTT
β-Catenin—F	CTGAAGAGGACCAGA
β-Catenin—R	TCCTTCTGCACACATTTGA
Twist-F	GACGGTTCGCCATCCAGAC
Twist-R	TGTCCATTTTCTCCTTCTCTGGA
Cyclin D1-F	GCTGCGAAGTGGAAACCATC
CyclinD1-R	GCTGCGAAGTGGAAACCATC

subsequently turned at a rate of 15,000 revolutions per minute for 5 min. The amount of protein detected was identified through the execution of the Bradford protein assay. First, the protein samples were separated using 12% SDS–PAGE. Then, they were transferred onto a polyvinylidene difluoride membrane. Following this, the membranes were immersed in a 5% skim milk solution as a means of blocking for a duration of 2 h. After coming into contact with anti-Caspase-3 (catalog #ab32351, Abcam), anti-Bcl2 (C-2; catalog #ab32124, Abcam), anti-Bax (catalog #ab182733, Abcam), and anti-VEGF (catalog #ab46154, Abcam), the blots were given the opportunity to interact overnight in a cooled environment at 4 °C. This was then followed by the addition of a secondary antibody for 2 h at normal room temperature. The bands were identified using the Pierce ECL detection reagent during the completion of the identification process. At this particular moment, the ImageJ Launcher software for imaging (version 1.48) available on the NCBI website was used to determine the density of each band.

Flow cytometry

The quantity of cell death, known as apoptosis, was precisely gauged by utilizing flow cytometry and the Annexin V-FITC Kit, provided by Exbio-Czech. A sum of 300,000 HCT116 cells were evenly dispersed among six wells on a plate. The cells were divided into five separate categories: those not treated, those treated with DOX, those treated with dendrimer G2, those treated with both dendrimer G2 and DOX, and those treated with both dendrimer and IF7, as well as DOX. Following a time period of 1 day, the cells were washed with PBS and subsequently stained with FITC-labeled Annexin V and PI.

Statistical analysis

The inquiry involved three back-to-back trials, with the outcome being determined by calculating the mean of the results from each of the three attempts. The information gathered in this research was analyzed using the SPSS program. The strategy of employing student's *t* test and one-way analysis of variance (ANOVA) test was employed to compare a variety of events. With the assistance of the statistical software GraphPad Prism, visual representations were generated, and a significance threshold of $P < 0.05$ was used to determine significance.

Results

Characterization of prepared formulations

To validate the production of nanoparticles and authenticate the attachment of functional groups on their outer layer, the method of FT-IR was utilized. The creation of G2, a linear globular dendrimer with negative characteristics, was achieved using citric acid to form strong bonds between the initial and subsequent generations of the dendrimer through C–O linkages. At a rate of 1232 cm^{-1}, these connections were noted. Furthermore, the occurrence of C=O bonds in the end citric acid units found in the dendrimer G2 was also identified at a wavelength of 1727 cm-1. Furthermore, the findings indicated a correlation at the 3300 cm^{-1} point, which corresponds to the stretching of O–H and N–H bonds. Furthermore, there was a noticeable increase in intensity at 1649 cm^{-1}, indicating the possible existence of an amide bond, as illustrated in Fig. 2.

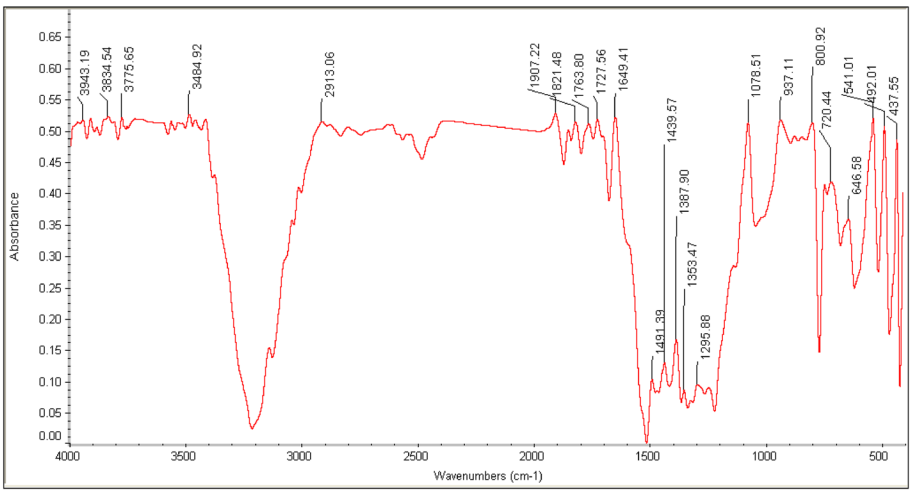

Fig. 2 FT-IR spectroscopy of anionic linear globular dendrimer G2 + peptide IF7

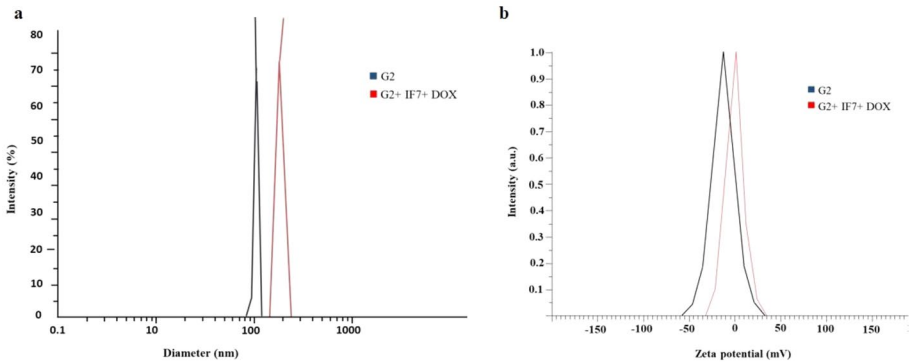

Fig. 3 DLS of dendrimer G2 + DOX + IF7 in comparison with intact dendrimer G2. **a** Size and (**b**) zeta potential distribution

This graph, represented in Fig. 3, depicts the implementation of DLS analysis to measure the distribution of particle sizes and the zeta potential. The primary purpose of this analysis was to ensure the suitability of dendrimer G2 + DOX + peptide IF7 as a delivery system for tumors. The mean size of dendrimer G2 was analyzed before and after the addition of the peptide and DOX to validate its effectiveness. Before being linked to a peptide, the dendrimer G2 measured 115.5 ± 15.2 nm and had a zeta potential of − 12.5 ± 1.5. Following the coupling procedure and addition of DOX, the size of the particles experienced a slight rise to 165.6 ± 24.6 nm, while the zeta potential shifted to − 0.3 ± 0.1.

TEM and FESEM were employed to precisely ascertain the physical composition of the formulations. According to the TEM pictures, it was confirmed that both the dendrimer and dendrimer G2 + DOX + Peptide IF7 formulas had a high level of uniformity, consistency, and a spherical structure. The average sizes of these particles were around 5.61 ± 1.56 nm and 7.63 ± 1.93 nm, as shown in Fig. 4. The results of the FESEM were in agreement with the observations made through DLS and TEM. The

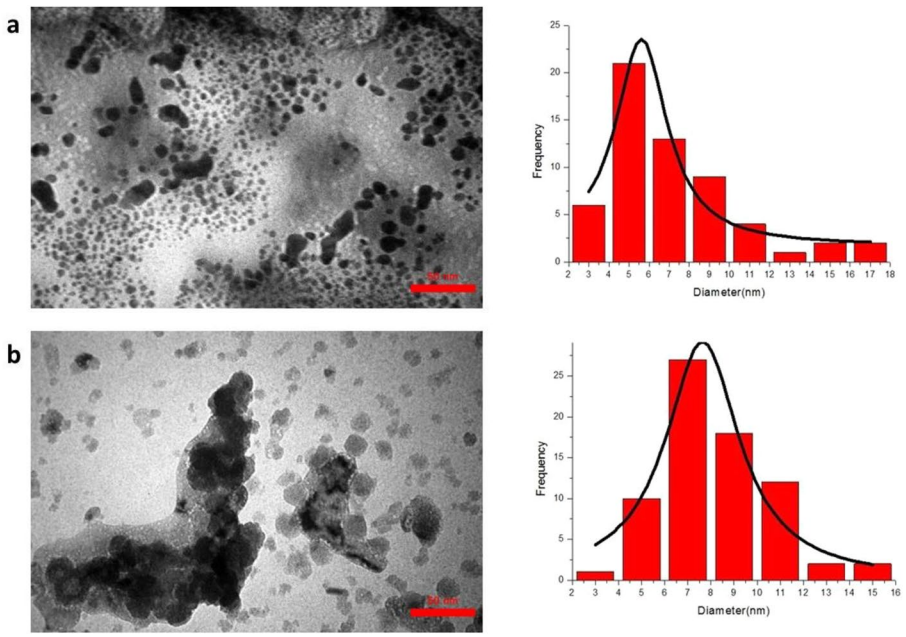

Fig. 4 TEM image and size distribution histogram of (**a**) dendrimer G2 and (**b**) dendrimer G2 + IF7 + DOX

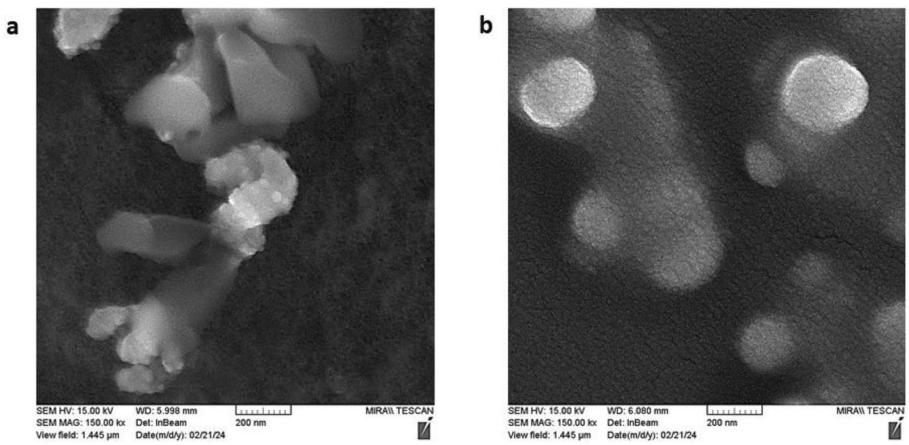

Fig. 5 FEEM image of (**a**) dendrimer G2 and (**b**) dendrimer G2 + IF7 + DOX

FESEM images clearly displayed the spherical shape of the particles in the prepared formulations (Fig. 5).

DOX loading and release

The estimated LE was about 61%. The dispensing of G2 + DOX + IF7 was examined at two distinct levels of acidity: pH 7.4 was replicated using PBS medium to mirror the typical tissue setting, while pH 5.5 was simulated to imitate the tumor's environment. After 48 h, the quantity of DOX released from dendrimer G2 + IF7 was evaluated in

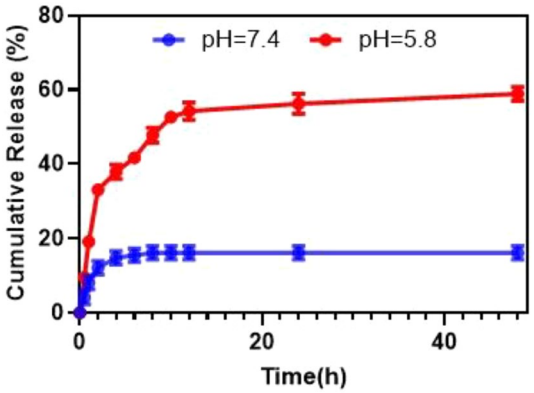

Fig. 6 Release profile of DOX from dendrimer G2 + IF7 + DOX nanoparticles at pH = 5.8 and pH = 7.4

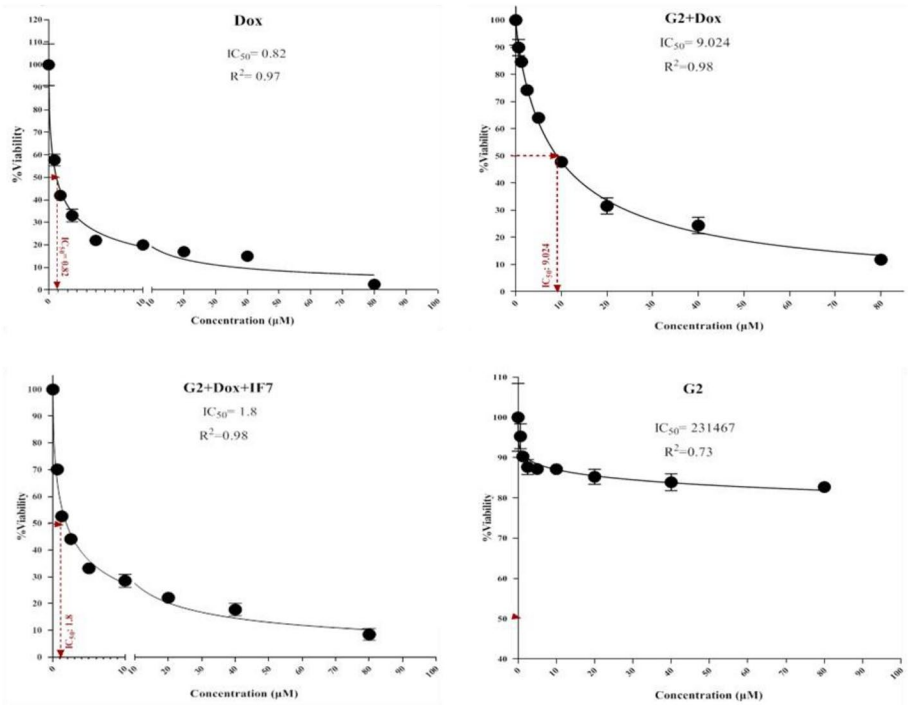

Fig. 7 MTT test results for DOX, dendrimer G2 + DOX, dendrimer G2 + DOX + IF7 and dendrimer G2 on HCT116 cells

solutions with a pH level of 5.5 and 7.4. Based on Fig. 6, the amount of DOX released at a pH of 5.5 was approximately 58%, a significant increase compared to the 16% released at a pH of 7.4.

The cytotoxicity effects of dendrimer G2 + peptide IF7

Each of the experimental groups showed a different level of influence on the survivability of HCT116 cells (ANXA1 positive), SW480 cells (ANXA1 negative), and HFF-2 cells (normal cells) with the strength of the effect being directly related to the dosage. As shown in Figs. 7, 8 and 9, all cell lines were more sensitive to DOX than G2 + DOX, and G2 + DOX + IF7. The amount of DOX present at which half of the cells were no longer

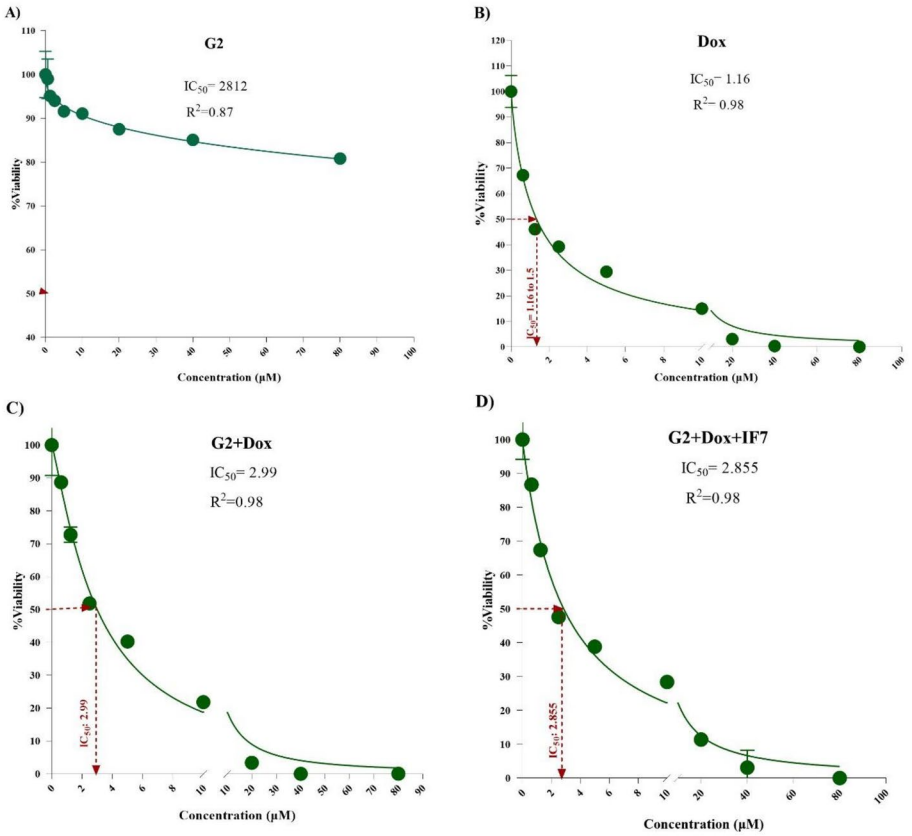

Fig. 8 MTT test results for DOX, dendrimer G2 + DOX, dendrimer G2 + DOX + IF7 and dendrimer G2 on SW480 cells

viable, also referred to as the IC50, was 0.82 and 1.16 μM in HCT116 and SW480 cells, respectively. For dendrimer G2 + DOX, the concentration required for a 50% reduction in cell viability was 9.02 μM in HCT116 cells, while for dendrimer G2 + DOX + IF7, it was 1.8 μM. However, the concentration required for a 50% reduction in cell viability for dendrimer G2 + DOX was approximately similar to dendrimer G2 + DOX + IF7 (2.99, and 2.85 μM, respectively) in SW480 cells (ANXA1 negative). The more potent cytotoxicity of dendrimer G2 + DOX + IF7 than dendrimer G2 + DOX in ANXA1-positive HCT116 cells shows the inference of ANXA1-mediated endocytosis and ANXA1-mediated transportation.

Importantly, DOX showed more cytotoxicity effects on the HFF-2 (normal cells). However, G2 + DOX + IF7 and dendrimer G2 + DOX showed significantly weaker cytotoxicities against HFF-2 cells, suggesting that the nanoformulations of DOX could improve the safety profile of DOX.

G2 + IF7 + DOX can inhibits the genes expression related to Wnt/β-catenin pathway

Gene expression analysis was conducted using RT-qPCR (displayed in Fig. 10) to measure the levels of cyclin D1, Twist, Zinc-finger E-box-binding homeobox 1 (ZEB1), and β-catenin in HCT116 cells. Once the cells were introduced to dendrimer G2, DOX was administered, followed by a mixture of dendrimer G2 and DOX, as well as a blend

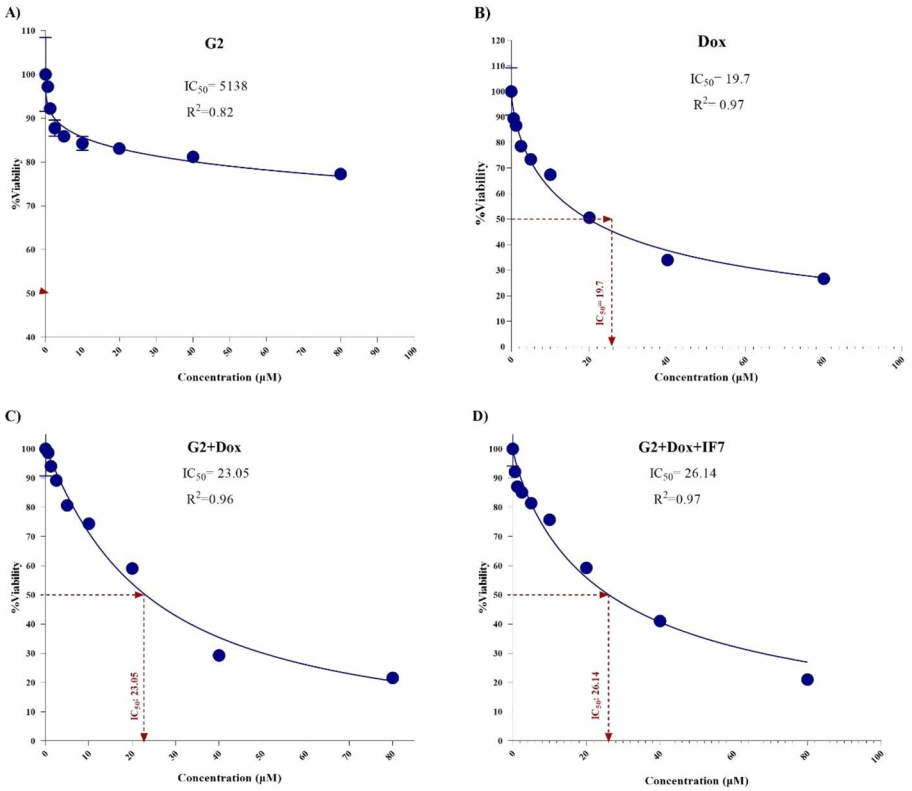

Fig. 9 MTT test results for DOX, dendrimer G2 + DOX, dendrimer G2 + DOX + IF7 and dendrimer G2 on normal cells

of dendrimer G2, peptide, and DOX. The outcomes showed that the administration of dendrimer G2 had no impact on the levels of ZEB1, cyclin D1, Twist, and β-catenin in comparison with the group that did not receive treatment. However, the application of DOX, along with the combination of dendrimer G2 + DOX and dendrimer G2 + DOX + IF7, led to significant inhibition of the expression of these genes ($p < 0.05$). Figure 10 shows that the combination treatment of dendrimer G2-peptide IF7 and DOX exhibited greater efficacy in reducing the expression of all four studied genes compared to G2, DOX alone and DOX + G2 groups. However, no statistically significant differences were observed between the dendrimer G2-peptide IF7 + DOX combination and the other treatment groups across all genes.

The effects of G2 + IF7 + DOX on the expression of proteins involved in apoptosis and angiogenesis in western blot

All three of the interventions, G2 + IF7 + DOX, G2 + DOX and DOX, led to higher concentrations of the caspase-3 ($p < 0.0001$) and Bax proteins ($p < 0.0001$), while there were lower levels of the Bcl-2 ($p < 0.0001$) and VEGF ($p < 0.05$) proteins compared to untreated group. The administration of G2 + IF7 + DOX had the most notable effect on the expression of proteins (as shown in Fig. 11).

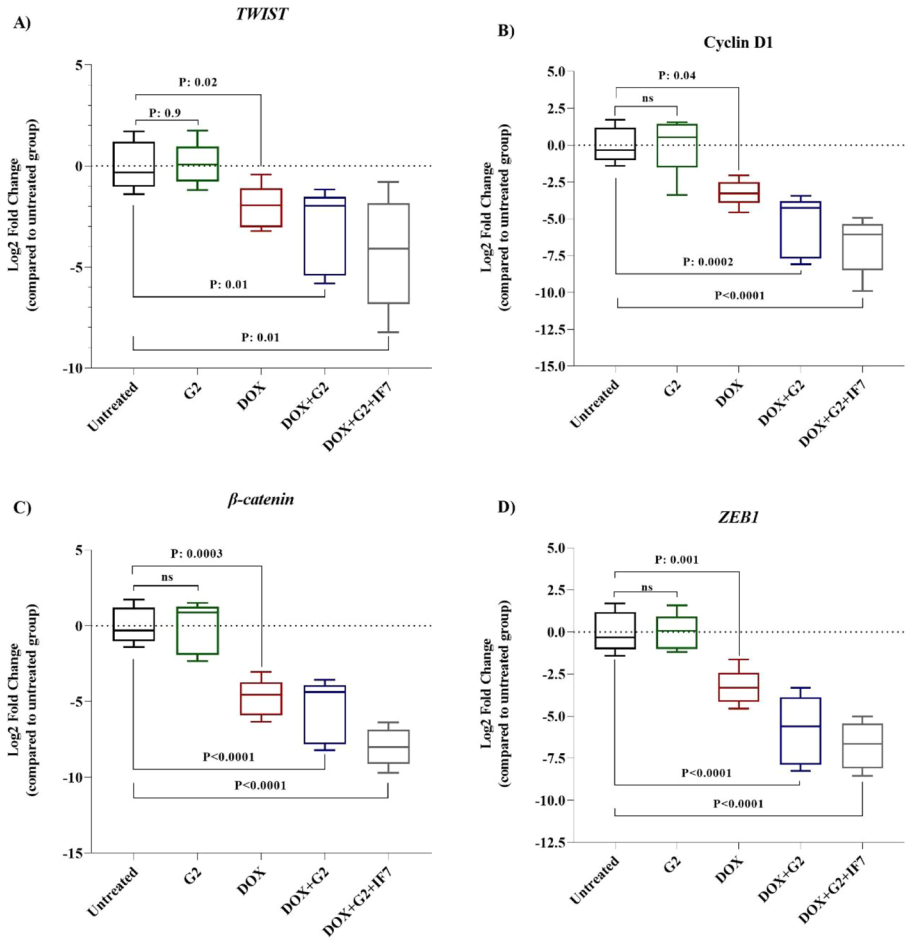

Fig. 10 Effects of dendrimer G2, doxorubicin (DOX), dendrimer G2 in combination with DOX, and dendrimer G2 combined with peptide IF7 and DOX on the gene expression of TWIST, Cyclin D1, β-catenin, and ZEB1 in HCT116 cells were examined. We used the ΔΔCt method to calculate the relative gene expression levels, and a one-way ANOVA test to compare the relative expression levels between the different treatment groups. The results are presented as mean ± SD fold change for the treatment groups: for TWIST, G2 was 0.10 ± 0.11, DOX − 2.10 ± 0.11, DOX + G2 − 3.18 ± 0.40, and DOX + G2 + IF7 − 4.30 ± 0.59; for Cyclin D1, G2 was 0.04 ± 0.33, DOX − 3.23 ± 0.15, DOX + G2 − 5.44 ± 0.42, and DOX + G2 + IF7 − 6.75 ± 0.36; for β-catenin, G2 was − 0.09 ± 0.33, DOX − 4.77 ± 0.22, DOX + G2 − 5.58 ± 0.42, and DOX + G2 + IF7 − 7.99 ± 0.19; and for ZEB1, G2 was − 0.02 ± 0.11, DOX −3.28 ± 0.11, DOX + G2 − 5.82 ± 0.40, and DOX + G2 + IF7 − 6.74 ± 0.29. The results indicate that all treatment combinations significantly downregulated the expression of these genes compared to controls, with *p* values confirming the statistical significance of the findings. These results suggest that the treatments could play an important role in regulating the expression of these critical oncogenes in colon cancer cells

The effects of G2 + IF7 + DOX on apoptosis rate in flow cytometry

The examination of Annexin V/PI staining through flow cytometry demonstrated a marked rise in the percentage of programmed cell death in cells exposed to different DOX formulations, G2 + IF7 + DOX, G2 + DOX and DOX, compared to those that were not treated ($p = 0.0002$, $p = 0.009$ and $p = 0.04$, respectively). The group that received Dendrimer G2 + peptide IF7 + DOX exhibited a significantly increased level of apoptosis in comparison with the remaining groups (as shown in Fig. 12).

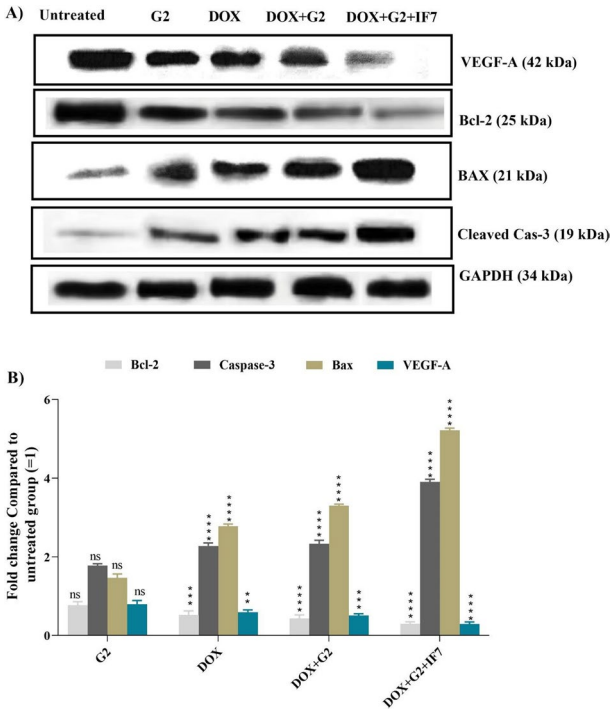

Fig. 11 Levels of Bcl-2, caspase-3, Bax and VEGF in DOX, dendrimer G2, dendrimer G2 + DOX and dendrimer G2 + DOX + IF7 treated HCT116 cells measured by Western blotting. The protein expression levels of Bcl-2, Caspase-3, Bax, and VEGF-A were analyzed in different study groups: G2, DOX, DOX + G2, and DOX + G2 + IF7, with the untreated controls serving as the baseline (fold change = 1). We used a one-way ANOVA test to compare the intensity of the bands between the different treatment groups. Quantitative data represent relative protein expression's mean ± standard deviation (SD). The expression levels were as follows: Bcl-2: G2 (0.77 ± 0.09), DOX (0.52 ± 0.10), DOX + G2 (0.44 ± 0.09), and DOX + G2 + IF7 (0.30 ± 0.05); Caspase-3: G2 (1.21 ± 0.05), DOX (2.28 ± 0.08), DOX + G2 (2.33 ± 0.09), and DOX + G2 + IF7 (3.91 ± 0.07); Bax: G2 (1.32 ± 0.10), DOX (2.78 ± 0.05), DOX + G2 (3.30 ± 0.04), and DOX + G2 + IF7 (5.22 ± 0.05); VEGF-A: G2 (0.79 ± 0.09), DOX (0.60 ± 0.06), DOX + G2 (0.51 ± 0.05), and DOX + G2 + IF7 (0.29 ± 0.05). Statistical significance was determined using Sidak's multiple comparisons test, with adjusted P values indicating significant differences (***$p < 0.001$, **$p < 0.01$, *$p < 0.05$) and ns indicating non-significant differences

Discussion

Based on reports, the dendrimer has become a notably successful approach for administering medication in the fight against cancer. The method offers multiple benefits, such as enhanced circulation and better capacity to contain medication (Sunoqrot et al. 2014; Elkin et al. 2015). Moreover, the intrinsic resistance to water within the internal environment also contributes to the capability of creating compounds and enclosing hydrophobic chemotherapy medications, ultimately resulting in greater water solubility and availability in the body. One method of preventing unintended harmful effects on cells and reducing drug toxicity, such as DOX, is by implementing this approach (Morgan et al. 2006; Morgan et al. 2003; Zhang et al. 2014a). Dendrimers from Generation 2 have significantly reduced levels of toxicity when compared to their preceding and subsequent generations (G1, G3, and G4) (Hsu et al. 2017). This research was focused on creating a G2 linear dendrimer with an anionic structure. This structure was composed of two crucial elements: a core based on polyethylene glycol (PEG) and branches made of citric acid. The PEG center of the dendrimer functions as a means of non-invasively transporting the drug to cancer cells. Meanwhile, the citric acid side

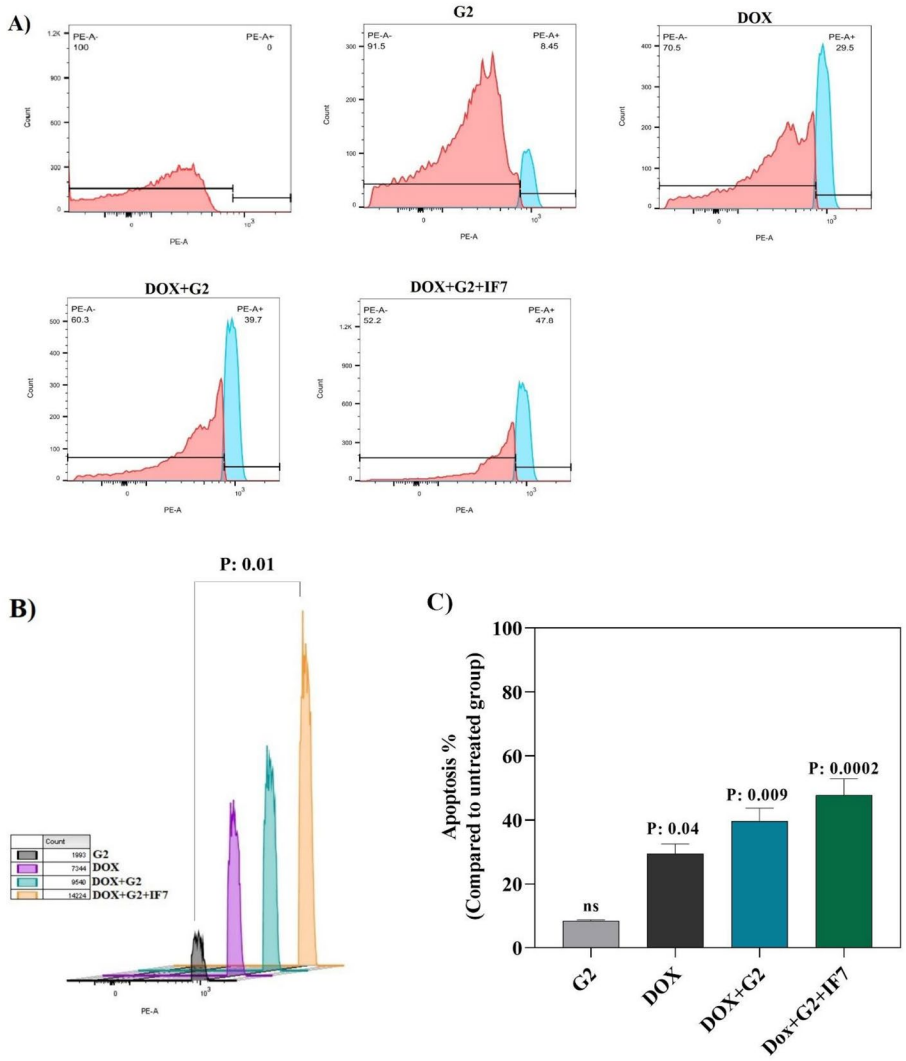

Fig. 12 Effects of DOX, dendrimer G2, dendrimer G2 + DOX and dendrimer G2 + DOX + IF7 on apoptosis. We used a two-way ANOVA test to compare the percentage of apoptotic cells between the different treatment groups. Statistical significance was determined using Sidak's multiple comparisons test, with adjusted P values indicating significant differences (***$p < 0.001$, **$p < 0.01$, *$p < 0.05$) and ns indicating non-significant differences

branches aid in breaking down the dendrimer and ensuring its removal from the body without harm (Astruc et al. 2010; Zhao et al. 2010; Cheng and Xu 2008). Furthermore, this specific particle has advantageous qualities such as the ability to biodegrade, minimal impact on organisms**,** economic production, and less detrimental impacts on the body in comparison with other polymers, such as polyamidoamine (PAMAM) (Pryor et al. 2014; Madaan et al. 2014; Alavidjeh et al. 2010; Hashempour Alamdari, et al. 2017). Earlier studies have shown that employing cancer treatment using nanocarriers derived from dendrimer G2 holds tremendous potential. To illustrate, a specific type of dendrimer called chlorambucil-conjugated PEG-based dendrimer G2 demonstrated the capability

to substantially inhibit the proliferation of breast cancer, fibrosarcoma, ovarian cancer, and CRC tumors by precisely honing in on them (Assadi 2016; Haririan 2010).

The methods utilized to analyze the physical and chemical characteristics of the nanoparticles indicated that they were of small dimensions and had the capacity to respond to changes in pH levels. Through the application of FT-IR, the conformation of dendrimer G2 and the linking of peptides were verified. This study determined that the hydrodynamic diameters of dendrimer G2 and dendrimer G2 + IF7 + DOX were below 200 nm, specifically measuring at 115.5 nm and 165.6 nm, respectively. However, the TEM findings indicated the smaller dimensions. The higher value of average size obtained in DLS (compared to TEM) arises, because DLS measures the hydrodynamic radii of the particles, which include the solvent layer at the interface. In contrast, the TEM was used for the formulation in a dehydrated state (Bhattacharjee 2016). The images from TEM and SEM, as previously observed, showed distinct nanoparticles with a uniform and circular morphology. Given the characteristics of dendrimers, the outcome was expected (Khodadust et al. 2013; Rouhollah et al. 2013). The agglomeration rate was low in the nanoparticles, which was also observed in FESEM images, as previously has been observed, the agglomeration can occur by the Van der Waals forces between the nanoparticles (Khodadust et al. 2013; Dung 2009). The calculated zeta potential of dendrimer G2 was around -12.5 ± 1.5 mV, likely due to the presence of citrate ions. Upon examining G2 + DOX + IF7, it was concluded that the zeta potential was measured at approximately − 0.4 mV. The rise in zeta potential could be due to the existence of peptide molecules that carry a positive charge and the presence of an amino group in DOX that can be protonated (Zanjanchi et al. 2022; Manocha and Margaritis 2010). The significant factor that allows DOX to be successfully loaded onto dendrimer G2, despite the dendrimer's negative charge, is the presence of a positive charge. This positive charge promotes electrostatic attraction between the two substances (Chandra et al. 2011). This characteristic allows for the connection and communication between dendrimers and IF7 in the present investigation. Alternatively, it can be stated that 59% of the medication was effectively incorporated into dendrimer G2 + IF7 and it was noted that this particular dendrimer was affected by variations in pH, facilitating the discharge of DOX. In particular, the speed at which DOX is discharged from the dendrimer G2 + IF7 + DOX mixture was observed to be faster at a pH value of 5.5 as opposed to a pH value of 7.4. The behavior of nanoparticles in acidic conditions is crucial, as human tumors often have an acidic pH (Vaupel 2004). Researchers are increasingly leveraging this acidic environment to enhance local drug concentrations while reducing systemic exposure. Nanoparticles (NPs) have been engineered for pH-sensitive drug release, utilizing structures that alter their physical and chemical characteristics in response to local pH variations. Specifically, these NPs react to the acidic pH present in tumor microenvironments. The mechanism of DOX release from dendrimers G2 + peptide IF7 could be explained based on the structural behavior of NPs and an ion exchange mechanism. Indeed, the existed amino groups of peptide IF7 in the dendrimer G2 at acidic pH are protonated by accepting H + ions, leading to positively charged $-NH_3+$ groups. When the branches of dendrimers are exposed to an acidic surrounding

and become protonated, the electrically charged particles may lead to a distance between them and the primary amine groups of DOX, as they both carry a positive charge. As a consequence, there may be a faster discharge of DOX from the dendrimer's hydrophobic core (Zhang et al. 2014b).

The use of dendrimer nanoparticles in passive targeting techniques has displayed potential in harnessing the enhanced permeability and retention (EPR) phenomenon for cancer treatment, thanks to their unique physical and chemical characteristics. However, recent studies suggest that this strategy may only be effective in treating stationary tumors with considerable permeability. However, the varied group of tumors in later stages of CRC presents uneven and insufficient permeability. Therefore, using specific ligands that target cancer cells has the potential to effectively solve the current problems (Rai et al. 2023). Consequently, the final and conclusive fusion of G2, IF7, and DOX was formed through the formation of a unique binding called peptide IF7. The peptide IF7 can effectively target ANXA1, a protein present in high amounts in cancerous cells like those found in colorectal cancer (Hatakeyama et al. 2011). Studies have demonstrated that utilizing nanoparticles loaded with chemotherapy drugs and linked to peptide IF7 may offer a specific approach for administering treatment to cancer cells characterized by a higher level of ANXA1 on their surface. Nanoparticles, treated with a particular IF7 peptide and combined with paclitaxel, have effectively hindered the advancement of breast tumors (Yu et al. 2015). The combined use of IF7 and paclitaxel, along with micelle nanoclusters, resulted in a much more pronounced inhibition of tumor growth in lung cancer models, compared to using micelle nanoclusters and paclitaxel separately (Oh et al. 2014). In addition, the compound IF7, composed of peptide-SN38, can penetrate the brain's protective barrier and successfully inhibit the growth of brain tumors in mice (Nonaka et al. 2020). A research project carried out on a live organism has revealed the unique cancer-fighting properties of peptide IF7. It was observed that when combined with SN-38, this peptide was highly effective in impeding the development of CRC HCT116 tumors, showing significant results within just 1 min of administration. Moreover, administering small amounts did not lead to any adverse effects (Hatakeyama et al. 2011).

Our results show that the IC50 measurement for dendrimer G2 + IF7 + DOX was greater compared to that of unbound DOX. Previous studies also demonstrated that the IC50 level of PEGylated dendrimer plus DOX, dendrimer G5-DOX, and enzyme-triggered PEGylated peptide dendrimer plus DOX was greater than that of free DOX (Zhang et al. 2014b; Zhang et al. 2014c; Kaminskas, et al. 2012). Through the process of diffusion, DOX is capable of easily crossing the cell membrane. The presence of a hydrophobic anthracycline compound greatly enhances the capacity of DOX to penetrate the cell membrane (Yacoub et al. 2011). Though the cell membrane's permeability to free DOX has its benefits, it also has its downsides, such as potentially causing non-specific cell death, especially in the heart, and potentially causing resistance to the drug, thus reducing its efficacy in cancer treatment (Yacoub et al. 2011; Al-Malky et al. 2020). The possibility of using nanocarriers to aid in endocytic pathways presents a promising solution for conquering and bypassing drug resistance mechanisms (Wong et al. 2006). The inclusion of nanoparticles containing G2 + DOX + IF7 can effectively alleviate these

limitations. The incorporation of the ANXA1-specific peptide onto the nanoparticles enhances their ability to attach to cancer cells that express ANXA1 (Liu et al. 2018). The interaction between IF7 and the first part of ANXA1 results in its transfer to cancer cells through three separate processes: clathrin-mediated endocytosis, caveolae-mediated endocytosis, and micropinocytosis (Hatakeyama et al. 2011; Oh et al. 2014). ANXA1's targeting peptide is highly adept at identifying and targeting cancer cells, effectively initiating internalization and allowing for a greater absorption of chemotherapy drugs like DOX into the cells (Liu et al. 2018).

According to our findings, when using G2 + DOX + IF7 nanoparticles, there is potential for negative effects on colorectal cancer cells through the regulation of apoptosis and the Wnt/β-catenin pathway. The results were achieved by reducing the expression of genes involved in β-catenin, cyclin D1, ZEB1, and Twist, and increasing cell death by increasing the levels of Bax and caspase-3 proteins while decreasing the levels of Bcl2 protein. In addition, the combination of G2, IF7, and DOX also hindered the synthesis of VEGF protein.

One of the main characteristics of colorectal cancer (CRC) is an aberrant regulation of cell death, leading to a decreased response to treatment. The increase in proteins related to apoptosis, like Bax and caspases, and the decrease in anti-apoptotic proteins like Bcl2, impede the ability to suppress the growth of tumors (Zhang and Yu 2013). VEGF is essential in the development of tumors, as it encourages the creation of fresh blood vessels and inhibits cell death through the promotion of Bcl-2 protein production (Pidgeon et al. 2001). Moreover, CRC displays an increased level of Twist, which is linked to the invasion of malignant tumors (Hong and Lim 2009). In addition, prior research has verified that increased amounts of Twist are linked to the spread of malignant tumors and the formation of new blood vessels (Fu et al. 2011). There are instances, where the Twist can result in an increase in β-catenin levels, triggering its functioning and causing it to relocate to the nucleus, in relation to colorectal cancer (Li and Zhou 2011; Lu et al. 2018; Oh et al. 2016). The Wnt-β-catenin signaling pathway plays a vital role in the progression of colon cancer (Suebsoonthron et al. 2017). Suppressing the β-catenin gene was effectively able to hinder the invasion of cancer cells by specifically hindering the production of Bclxl, X-linked inhibitor of apoptosis (XIAP), and nuclear p65 (Zhang et al. 2011). By stopping the activity of β-catenin, the ability of cancer cells to migrate was hindered (Han et al. 2013). β-catenin/transcription factor 4 (TCF4)'s direct participation in the ZEB1 promoter initiates the initiation of transcription ZEB1 plays a crucial role in triggering epithelial-to-mesenchymal transition (EMT), which ultimately promotes tumor growth in CRC (Sánchez-Tilló et al. 2011). Furthermore, in the realm of CRC, β-Catenin appears to have a positive impact on promoting the expression of cyclin D1 (Shtutman et al. 1999). The protein functions as a regulatory element that controls the function of cyclin-dependent kinase 4/6, fostering the shift from G1 to S phases during cell division and promoting the growth of cancer cells (Qie and Diehl 2016).

Research has demonstrated the anticancer effects of nanoparticles containing DOX. The use of a conjugate of DOX and transferrin leads to cell death by blocking the Wnt/β-catenin signaling pathway (Szwed et al. 2015). The inclusion of folic acid in DOX–albumin nanoparticles successfully obstructed the Wnt/β-catenin pathway, leading

to the inhibition of precancerous growths in gastric cancer (Yan et al. 2023). A new technique has been discovered by scientists that aims to enhance the effectiveness of DOX for treating breast cancer. This involves the use of specialized nanoparticles that specifically target the Frizzled7 protein and primarily work on the Wnt/β-catenin pathway (Hoover et al. 2024). Furthermore, the utilization of zymosan nanoparticles loaded with DOX resulted in the suppression of genes associated with the Wnt/β-catenin pathway (such as Twist, cyclin D1, and ZEB1) and promoted the induction of colon cancer cell death (Rajabi et al. 2024). Numerous scientific studies have also substantiated the deleterious effects of dendrimer–DOX nanoparticles, as they possess the capacity to precisely influence the mechanisms responsible for cell death, commonly referred to as apoptosis. The dendrimer was able to greatly enhance the absorption of DOX, resulting in a considerable increase in effectiveness compared to unbound DOX. This was evident in the results of the caspase 3 and 7 assay (Almuqbil et al. 2020). When it comes to breast cancer cells, the addition of DOX to the fourth iteration of dendrimeric nanoparticles greatly impacted the levels of gene expression related to apoptosis. More precisely, it caused an increase in the activity of genes that promote cell death, such as Puma, Noxa, and Bax while simultaneously reducing the levels of genes that prevent cell death, such as Apollon, Survivin, and BCL-2 (Khodadust et al. 2020). The combination of dendrimer and DOX in nanoparticles results in a notable increase in the production of cathepsin B, which consequently leads to elevated levels of caspase-3 and ROS while decreasing levels of Bcl-2. Hence, this leads to a heightened activation of cell death through lysosomal pathways in contrast to using DOX in its unattached state (Wang et al. 2020). Dendrimer containing Twist inhibitor also significantly inhibited metastasis by inhibition of TWIST-mediated expression of EMT target genes (Finlay et al. 2015). While the study provides valuable insights into the potential therapeutic applications of Peptide IF7-conjugated dendritic nanoparticles loaded with doxorubicin for targeting colorectal cancer, several limitations should be considered. First, the research was limited to in vitro experiments, and the results may not fully translate to in vivo conditions. The tumor microenvironment in living organisms can significantly influence drug delivery and efficacy, which was not accounted for in this study. Moreover, the study did not include assessments of the cellular uptake of the nanoparticles or the specific mechanisms of nanoparticle–drug internalization and trafficking within the cancer cells. These processes can critically impact the effectiveness of the treatment. The diversity in genetic and phenotypic profiles of colorectal cancer across different patient populations was also not explored, potentially limiting the generalizability of the findings. Furthermore, the investigation did not thoroughly address the long-term safety and potential toxicity of the nanoparticle formulation, particularly in non-targeted tissues. Future research should involve in vivo studies to validate these findings and assess any off-target effects, along with comprehensive studies on the cellular uptake mechanisms and the pharmacokinetics and pharmacodynamics of the nanoparticle system in a complex biological setting. Addressing these limitations will be crucial for fully understanding and optimizing the potential of Peptide IF7-conjugated dendrimers in clinical applications.

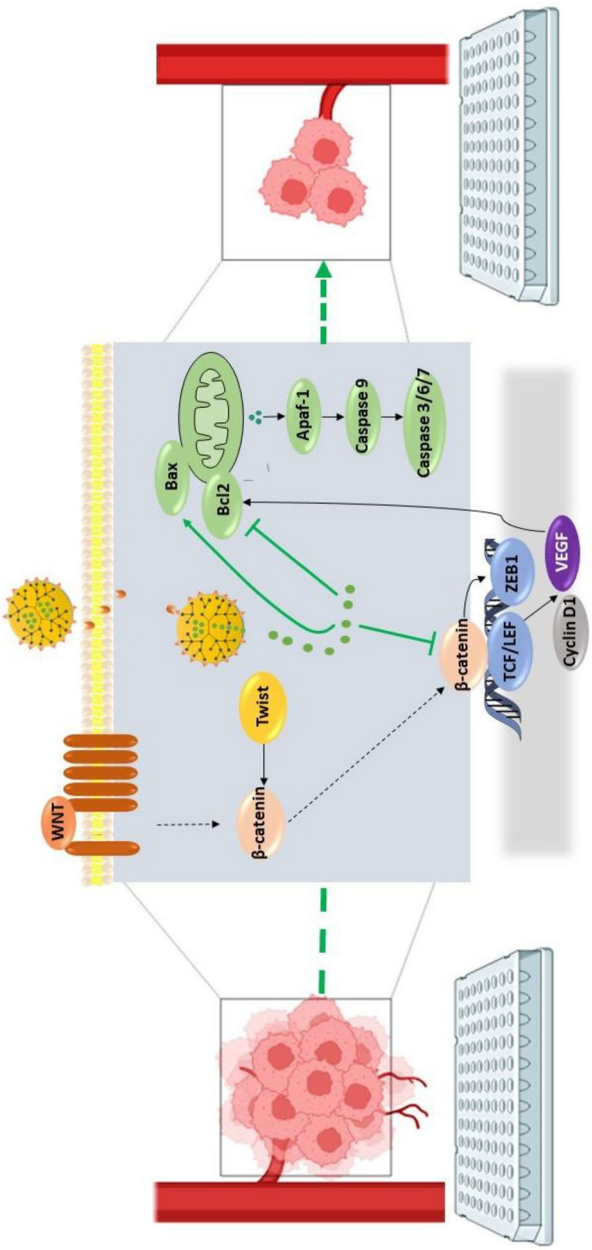

Fig. 13 Schematic representation of the effects of peptide IF7-conjugated dendrimer loaded with doxorubicin on different signaling pathways in HCT116 colorectal cancer cells

Conclusions

Incorporating Peptide IF7 into dendrimer G2 to form nanocarriers for DOX has the capability to enhance drug delivery by precisely targeting cells according to their pH levels. Early findings have indicated encouraging levels of cell-killing effects, potentially attributable to the selective focus on the Wnt/β-catenin and apoptosis mechanisms (see Fig. 13). Additional studies are needed to thoroughly comprehend the characteristics of this composition and its ability to effectively treat cancer.

Acknowledgements
The authors acknowledge the grant support of Tehran University of Medical Sciences, Tehran, Iran.

Author contributions
Omid Reza Tamtaji: Investigation (lead); methodology (equal); writing—original draft (equal). Mehdi Shafiee Ardestani, and Abdolkarim Talebi Taheri, Tina Rahjoo: Data curation (supporting); original draft, formal analysis (supporting); investigation (supporting), critical revised. Michael R Hamblin: Critical revised, writing—review and editing (equal). Hamed Mirzaei and Fatemeh Nabavizadeh: Conceptualization (equal); funding acquisition (lead); investigation (lead); resources (equal); supervision (equal); writing—review and editing (equal). All authors confirmed the final version of manuscript.

Funding
This study was supported by Vice Chancellor for Research (Grant No. 1401-3-233-62974), Tehran University of Medical Sciences, Tehran, Iran.

Availability of data and materials
The primary data for this study is available from the authors on direct request.

Declarations

Ethics approval and consent to participate
None.

Consent for publication
None.

Competing interests
The authors declare no competing interests.

Received: 20 July 2024 Accepted: 24 February 2025
Published online: 08 March 2025

References

Abbasi E et al (2014) Dendrimers: synthesis, applications, and properties. Nanoscale Res Lett 9:1–10
Alavidjeh MS et al (2010) Anionic linear-globular dendrimers: biocompatible hybrid materials with potential uses in nanomedicine. J Mater Sci Mater Med 21:1121–1133
Al-Malky HS, Al Hathi SE, Osman M-MM (2020) Major obstacles to doxorubicin therapy: cardiotoxicity and drug resistance. J Oncol Pharm Pract 26(2):434–444
Almuqbil RM et al (2020) Dendrimer conjugation enhances tumor penetration and efficacy of doxorubicin in extracellular matrix-expressing 3D lung cancer models. Mol Pharm 17(5):1648–1662
Assadi A et al (2016) Novel chlorambucil-conjugated anionic linear-globular PEG-based second-generation dendrimer: in vitro/in vivo improved anticancer activity. OncoTargets Thera 9:5531–5543
Astruc D, Boisselier E, Ornelas C (2010) Dendrimers designed for functions: from physical, photophysical, and supramolecular properties to applications in sensing, catalysis, molecular electronics, photonics, and nanomedicine. Chem Rev 110(4):1857–1959
Barot S et al (2024) Combined associations of a healthy lifestyle and body mass index with colorectal cancer recurrence and survival: a cohort study. Cancer Causes Control 35(2):367–376
Bhattacharjee S (2016) DLS and zeta potential–what they are and what they are not? J Control Release 235:337–351
Biaoxue R et al (2012) Upregulation of Hsp90-beta and annexin A1 correlates with poor survival and lymphatic metastasis in lung cancer patients. J Exp Clin Cancer Res 31:1–14
Boopathy LK et al (2024) Potential molecular mechanisms of myrtenal against colon cancer: a systematic review. J Biochem Mol Toxicol 38(1):e23525
Chandra S et al (2011) Dendrimer–doxorubicin conjugate for enhanced therapeutic effects for cancer. J Mater Chem 21(15):5729–5737
Cheng Y, Xu T (2008) The effect of dendrimers on the pharmacodynamic and pharmacokinetic behaviors of non-covalently or covalently attached drugs. Eur J Med Chem 43(11):2291–2297
Corrie PG (2008) Cytotoxic chemotherapy: clinical aspects. Medicine 36(1):24–28

Dung TT et al. Preparation and characterization of magnetic nanoparticles coated with polyethylene glycol. J Phys Conf Ser. 2009. IOP Publishing.
Elkin I, Rabanel JM, Hildgen P (2015) Influence of hydrophobic dendrimer core structure on the itraconazole encapsulation efficiency. Macromol Chem Phys 216(24):2356–2367
Finlay J et al (2015) RNA-based TWIST1 inhibition via dendrimer complex to reduce breast cancer cell metastasis. Biomed Res Int 2015(1):382745
Fu J et al (2011) The TWIST/Mi2/NuRD protein complex and its essential role in cancer metastasis. Cell Res 21(2):275–289
Han R et al (2013) Activation of β-catenin signaling is critical for doxorubicin-induced epithelial–mesenchymal transition in BGC-823 gastric cancer cell line. Tumor Biol 34:277–284
Haririan I, et al. Anionic linear-globular dendrimer-cis-platinum (II) conjugates promote cytotoxicity in vitro against different cancer cell lines. Int J Nanomed. 2010: 63–75.
Hashempour Alamdari N et al (2017) Gd 3+-asparagine-anionic linear globular dendrimer second-generation G2 complexes: novel nanobiohybrid theranostics. Contrast Media Mol Imaging 2017:1–19
Hatakeyama S et al (2009) Identification of mRNA splicing factors as the endothelial receptor for carbohydrate-dependent lung colonization of cancer cells. Proc Natl Acad Sci 106(9):3095–3100
Hatakeyama S et al (2011) Targeted drug delivery to tumor vasculature by a carbohydrate mimetic peptide. Proc Natl Acad Sci 108(49):19587–19592
Hong R, Lim SC (2009) Overexpression of Twist in colorectal adenocarcinoma. Basic Appl Pathol 2(1):15–20
Hoover EC et al (2024) FZD7-targeted nanoparticles to enhance doxorubicin treatment of triple-negative breast cancer. ACS Omega 9(12):14323–14335
Hsu HJ et al (2017) Dendrimer-based nanocarriers: a versatile platform for drug delivery. Wiley Interdiscip Rev Nanomed Nanobiotechnol 9(1):e1409
Kaminskas LM et al (2012) A comparison of changes to doxorubicin pharmacokinetics, antitumor activity, and toxicity mediated by PEGylated dendrimer and PEGylated liposome drug delivery systems. Nanomed Nanotechnol Biol Med 8(1):103–111
Kato I, Sun J (2023) Microbiome and diet in colon cancer development and treatment. Cancer J 29(2):89–97
Khodadust R et al (2013) PAMAM dendrimer-coated iron oxide nanoparticles: synthesis and characterization of different generations. J Nanopart Res 15:1–13
Khodadust R et al (2020) Poly (I: C)-and doxorubicin-loaded magnetic dendrimeric nanoparticles affect the apoptosis-related gene expressions in MCF-7 cells. Turk J Biol 44(4):133–144
Li J, Zhou BP (2011) Activation of β-catenin and Akt pathways by Twist are critical for the maintenance of EMT associated cancer stem cell-like characters. BMC Cancer 11:1–11
Liu Y et al (2018) Combination drug delivery via multilamellar vesicles enables targeting of tumor cells and tumor vasculature. Biotechnol Bioeng 115(6):1403–1415
Lu K, Dong J-L, Fan W-J. Twist1/2 activates MMP2 expression via binding to its promoter in colorectal cancer. Eur Rev Med Pharmacol Sci. 2018; 22(23).
Lüpertz R et al (2010) Dose-and time-dependent effects of doxorubicin on cytotoxicity, cell cycle and apoptotic cell death in human colon cancer cells. Toxicology 271(3):115–121
Madaan K et al (2014) Dendrimers in drug delivery and targeting: Drug-dendrimer interactions and toxicity issues. Journal of Pharmacy and Bioallied Sciences 6(3):139–150
Manocha B, Margaritis A (2010) Controlled release of doxorubicin from doxorubicin/γ-polyglutamic acid ionic complex. J Nanomater 2010:1–8
Minotti G et al (2004) Anthracyclines: molecular advances and pharmacologic developments in antitumor activity and cardiotoxicity. Pharmacol Rev 56(2):185–229
Mohammadzadeh P et al (2017) AS1411 aptamer-anionic linear globular dendrimer G2-Iohexol selective nano-theranostics. Sci Rep 7(1):11832
Morgan MT et al (2003) Dendritic molecular capsules for hydrophobic compounds. J Am Chem Soc 125(50):15485–15489
Morgan MT et al (2006) Dendrimer-encapsulated camptothecins: increased solubility, cellular uptake, and cellular retention affords enhanced anticancer activity in vitro. Can Res 66(24):11913–11921
Namazi H, Adeli M (2005) Dendrimers of citric acid and poly (ethylene glycol) as the new drug-delivery agents. Biomaterials 26(10):1175–1183
Nonaka M et al (2020) Overcoming the blood–brain barrier by Annexin A1-binding peptide to target brain tumours. Br J Cancer 123(11):1633–1643
Oh P et al (2014) In vivo proteomic imaging analysis of caveolae reveals pumping system to penetrate solid tumors. Nat Med 20(9):1062–1068
Oh BY et al (2016) Twist1-induced epithelial-mesenchymal transition according to microsatellite instability status in colon cancer cells. Oncotarget 7(35):57066
Okano M et al (2015) Upregulated Annexin A1 promotes cellular invasion in triple-negative breast cancer. Oncol Rep 33(3):1064–1070
Pidgeon GP et al (2001) Vascular endothelial growth factor (VEGF) upregulates BCL-2 and inhibits apoptosis in human and murine mammary adenocarcinoma cells. Br J Cancer 85(2):273–278
Pryor JB, Harper BJ, Harper SL. Comparative toxicological assessment of PAMAM and thiophosphoryl dendrimers using embryonic zebrafish. Int J Nanomed. 2014;1947–1956.
Qie S, Diehl JA (2016) Cyclin D1, cancer progression, and opportunities in cancer treatment. J Mol Med 94:1313–1326
Rai DB et al (2023) Dendrimer-mediated delivery of anticancer drugs for colon cancer treatment. Pharmaceutics 15(3):801
Rajabi A et al (2024) Doxorubicin-loaded zymosan nanoparticles: synergistic cytotoxicity and modulation of apoptosis and Wnt/β-catenin signaling pathway in C26 colorectal cancer cells. Int J Biol Macromol 260:128949
Rastogi V et al (2024) Dendrimer as nanocarrier for drug delivery and drug targeting therapeutics: a fundamental to advanced systematic review. Int J Polym Mater Polym Biomater 73(4):310–332

Ravizza R et al (2004) Role of the p53/p21 system in the response of human colon carcinoma cells to doxorubicin. BMC Cancer 4:1–10
Rouhollah K et al (2013) Doxorubicin loading, release, and stability of polyamidoamine dendrimer-coated magnetic nanoparticles. J Pharm Sci 102(6):1825–1835
Sánchez-Tilló E et al (2011) β-catenin/TCF4 complex induces the epithelial-to-mesenchymal transition (EMT)-activator ZEB1 to regulate tumor invasiveness. Proc Natl Acad Sci 108(48):19204–19209
Shtutman M et al (1999) The cyclin D1 gene is a target of the β-catenin/LEF-1 pathway. Proc Natl Acad Sci 96(10):5522–5527
Su N et al (2010) Increased expression of annexin A1 is correlated with K-ras mutation in colorectal cancer. Tohoku J Exp Med 222(4):243–250
Suebsoonthron J et al (2017) Inhibition of WNT signaling reduces differentiation and induces sensitivity to doxorubicin in human malignant neuroblastoma SH-SY5Y cells. Anticancer Drugs 28(5):469–479
Sunoqrot S et al (2014) Prolonged blood circulation and enhanced tumor accumulation of folate-targeted dendrimer-polymer hybrid nanoparticles. J Control Release 191:115–122
Szwed M, Kania KD, Jozwiak Z (2015) Toxicity of doxorubicin-transferrin conjugate is connected to the modulation of Wnt/β-catenin pathway in human leukemia cells. Leuk Res 39(10):1096–1102
Tacar O, Sriamornsak P, Dass CR (2013) Doxorubicin: an update on anticancer molecular action, toxicity and novel drug delivery systems. J Pharm Pharmacol 65(2):157–170
Vaupel P (2004) Tumor microenvironmental physiology and its implications for radiation oncology. Semin Radiat Oncol. 14:198
Victoir B et al (2024) Targeted therapeutic strategies for the treatment of cancer. Cancers 16(2):461
Wang J et al (2020) DOX-loaded peptide dendritic copolymer nanoparticles for combating multidrug resistance by regulating the lysosomal pathway of apoptosis in breast cancer cells. J Mater Chem B 8(6):1157–1170
Wang T et al (2024) Role of mitochondria in doxorubicin-mediated cardiotoxicity: from molecular mechanisms to therapeutic strategies. Cell Stress Chaperones 29:349
Wong HL et al (2006) A mechanistic study of enhanced doxorubicin uptake and retention in multidrug resistant breast cancer cells using a polymer-lipid hybrid nanoparticle system. J Pharmacol Exp Ther 317(3):1372–1381
Xi Y, Xu P (2021) Global colorectal cancer burden in 2020 and projections to 2040. Transl Oncol 14(10):101174
Yacoub TJ, Reddy AS, Szleifer I (2011) Structural effects and translocation of doxorubicin in a DPPC/Chol bilayer: the role of cholesterol. Biophys J 101(2):378–385
Yan F et al (2023) Fabrication of doxorubicin nanoparticles mediated by folic acid and its effect on the Wnt/β-catenin signaling to improve precancerous lesions in gastric cancer. Sci Adv Mater 15(1):79–87
Yang H (2016) Targeted nanosystems: advances in targeted dendrimers for cancer therapy. Nanomed Nanotechnol Biol Med 12(2):309–316
Yu D-H et al (2015) IF7-conjugated nanoparticles target Annexin 1 of tumor vasculature against P-gp mediated multidrug resistance. Bioconjug Chem 26(8):1702–1712
Zanjanchi P et al (2022) Conjugation of VEGFR1/R2-targeting peptide with gold nanoparticles to enhance antiangiogenic and antitumoral activity. J Nanobiotechnol 20(1):7
Zhang L, Yu J (2013) Role of apoptosis in colon cancer biology, therapy, and prevention. Curr Colorectal Cancer Rep 9:331–340
Zhang F et al (2011) SiRNA-mediated silencing of beta-catenin suppresses invasion and chemosensitivity to doxorubicin in MG-63 osteosarcoma cells. Asian Pac J Cancer Prev 12(1):239–245
Zhang C et al (2014a) Peptide dendrimer–doxorubicin conjugate-based nanoparticles as an enzyme-responsive drug delivery system for cancer therapy. Adv Healthcare Mater 3(8):1299–1308
Zhang M et al (2014b) Impact of dendrimer surface functional groups on the release of doxorubicin from dendrimer carriers. J Phys Chem B 118(6):1696–1706
Zhang C et al (2014c) Dendrimer–doxorubicin conjugate as enzyme-sensitive and polymeric nanoscale drug delivery vehicle for ovarian cancer therapy. Polym Chem 5(18):5227–5235
Zhao L et al (2010) High-throughput screening of dendrimer-binding drugs. J Am Chem Soc 132(38):13182–13184

Publisher's Note